JTTEE5 2:31-34

Degradation of Bond Coat Strength under Thermal Cycling—Technical Note

H. Wang and W. Montasser

Degradation in bond strength of plasma-sprayed thermal barrier coatings under thermal cycling was evaluated by tensile adhesion tests. The bond strength and failure mode for two types of bond coat materials were examined. Two bond coats having the same substrate and top ceramic coat behaved differently due to differences in the thermal mismatch stress at an interface between the metallic bond coat and the ceramic top coat.

1. Introduction

THE tensile adhesion test (ASTM C633-79) has been used extensively as a quality control procedure to assess adhesive/cohesive strength of thermally sprayed coatings.[1] The coating failure mode in this test could be cohesive (fracture occurs in the coating), adhesive (fracture occurs at the coating/substrate interface), or a mixture of the two. The test is performed at room temperature due to high-temperature limitations of epoxies, which bond a coating to a tensile test fixture. Therefore, such measurements, in general, have no direct relevance to high-temperature performance of thermal barrier coatings (TBC).

Thermal cycling tests, on the other hand, have been used to evaluate performance of plasma-sprayed thermal barrier coatings in a high-temperature environment.[2] In these tests, thermal barrier coating samples are generally heated by electrical furnaces or a flame torch and are quenched in air or water. The interaction between water and ceramic coatings increases the degree of thermal shock and shortens the thermal cycling lifetime of thermal barrier coatings.[3] The number of thermal cycles to coating failure usually is defined as the thermal cycling lifetime, and coating failure is inspected by either the unaided eye or by low-magnification optical microscopy. Because the samples are generally free from an external load, the sample failure caused by initiation and propagation of cracks normally is attributed to thermal mismatch between coating and substrate and/or phase changes due to oxidation of the metallic components.

In the present study, the above two tests were combined. Samples were subjected to tensile adhesion tests after a fixed number of thermal cycles. Thermal barrier coating degradation was evaluated by comparing the bond strength and the failure mode of thermal cycled samples against reference samples. The test results provide additional information on thermal barrier coating performance, which could not be obtained by the above-mentioned two tests individually, particularly for the thermal barrier coatings in-service with an external load.

Keywords: coefficient of thermal expansion (CTE), tensile adhesion tests, thermal barrier coatings (TBCs), thermal cycling, yttria stabilized zirconia

H. Wang and **W. Montasser**, Sherritt Gordon Limited, Fort Saskatchewan, Alberta, Canada.

2. Experimental Procedure

Two sets of thermal barrier coating samples with three samples in each set were subjected to the combined thermal cycling and tensile adhesion tests. The third set of samples was only subjected to tensile adhesion tests without thermal cycling and was used as a reference. The samples were manufactured in such a way that the bond coats, either Ni-Cr(19wt%)-Al(6wt%) alloy or a composite of Ni-Cr(4wt%)-Al(4wt%) alloy and 21wt% of alumina-silicate(bentonite), were air plasma-sprayed onto one end of a Hastelloy X (HX) cylindrical substrate, and magnesia(24wt%)-stabilized zirconia was subsequently sprayed onto the bond coats. The presence of alumina-silicate in the nickel-based alloy would reduce the overall thermal expansion of the bond coat, resulting in less mismatch with the magnesia-stabilized zirconia coating during thermal cycling. All of the coatings were applied by plasma spraying using a Metco 9MB gun. The cylindrical substrates had a diameter of 25.4 mm and height of 25 mm. The dimensions and components of these samples are listed in Table 1.

Table 1 Thermal barrier coating components, composition (wt%), thermal cycles, and dimensions

	Top coat	Bond coat	Substrate	Cycles
Set 1	ZrO_2-MgO(24%)	NiCr(19%)Al(6%)	Hastelloy X	100
Set 2	ZrO_2-MgO(24%)	NiCr(4%)Al(4%)/bentonite(21%)	Hastelloy X	100
Set 3	ZrO_2-MgO(24%)	NiCr(19%)Al(6%)	Hastelloy X	0
Coating				
Thickness, mm	0.60	0.25	25	...
Area, mm^2	160	160	160	...

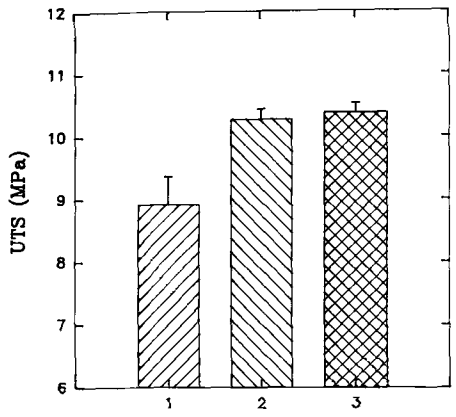

Fig. 1 Mean ultimate tensile stress and standard deviation for samples in Set 1 (No. 1) and Set 2 (No. 2) after 100 thermal cycles, and uncycled reference samples in Set 3 (No. 3).

Thermal cycling tests were carried out in an apparatus where the samples were heated to about 960 °C by a natural gas/air torch and then quenched by a cold water stream at 20 °C. The samples were cycled between the heating position for 10 min and the quenching position for 2 min. Each sample was thermally cycled 100 times.

The samples after thermal cycling were subjected to tensile adhesion tests according to ASTM C633-79. Subsequently, fracture surfaces of the samples were examined under a scanning electron microscope (SEM) equipped with energy-dispersive X-ray analysis capability (EDAX). The roughness of the fracture surfaces was measured by a surface profilometer. The bond coat materials were compacted and sintered, and the coefficients of thermal expansion were subsequently measured by a dilatometer from room temperature to 1030 °C at a heating rate of 10 °C/min in argon atmosphere.

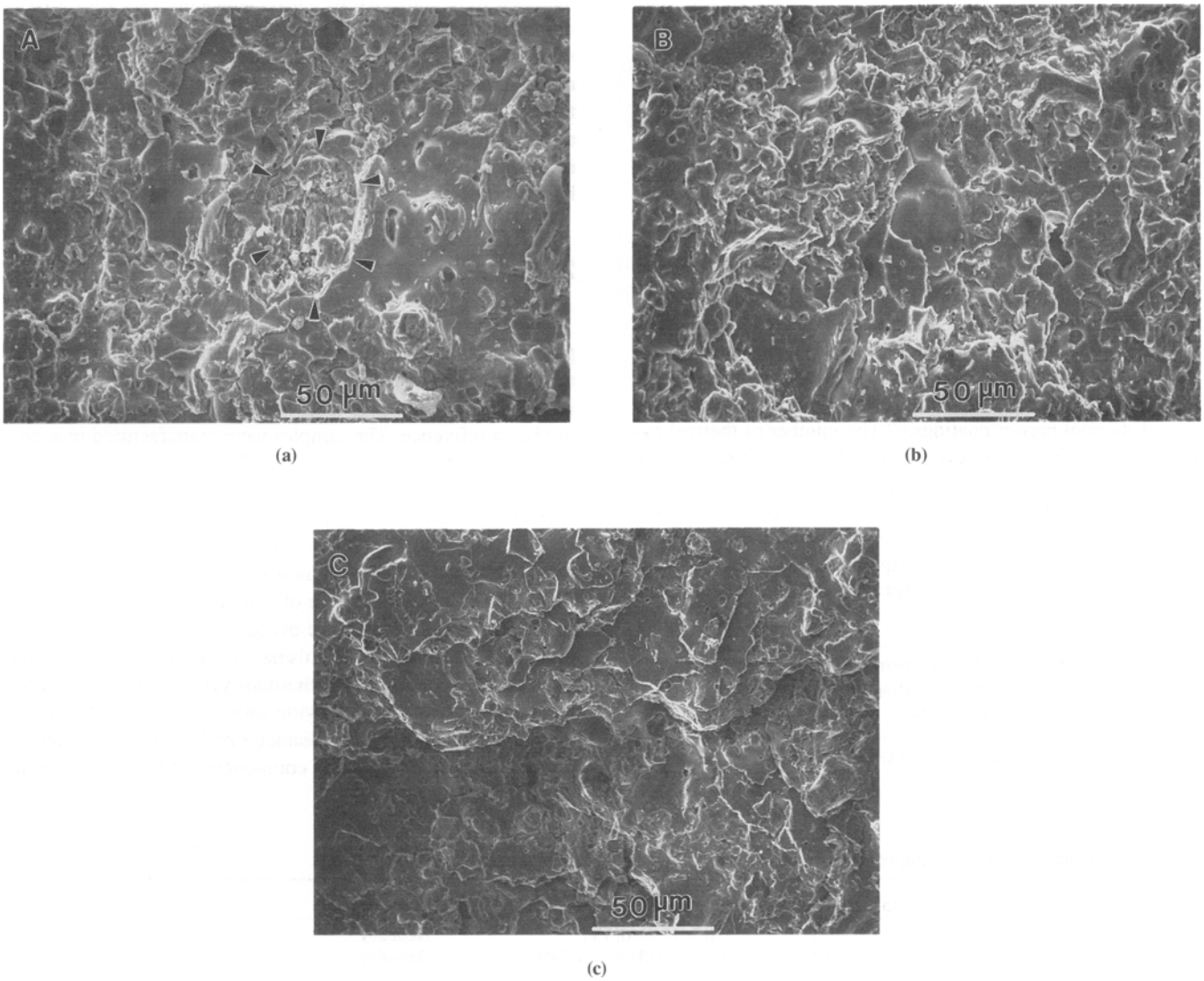

Fig. 2 Scanning electron micrographs of fracture surfaces after tensile adhesion tests for the samples in Set 1 (a), Set 2 (b), and Set 3 (c), showing more localized tearing in Sets 1 and 2. The bond coat elements nickel, chromium, and aluminum were detected by EDAX for the samples in Set 1, as indicated by the arrows in Fig. 2(a).

3. Results and Discussion

No macrocracks were observed after thermal cycling of these samples. The average ultimate tensile strength and standard deviation for samples in Sets 1 and 2 after 100 thermal cycles are shown in Fig. 1. Also shown are results of the tensile strength of the reference samples in Set 3 without thermal cycling. The failure mode of the samples in Sets 2 and 3 was found to be cohesive, i.e., the fracture occurred within the top ceramic coating. There is no significant difference in the ultimate tensile stress between the samples in Sets 2 and 3. The ultimate tensile stresses are 10.3 ± 0.3 MPa and 10.4 ± 0.3 MPa for the samples in Sets 2 and 3, respectively. However, the ultimate tensile stress of the samples in Set 1 is 8.9 ± 0.8 MPa after 100 thermal cycles. The fracture surfaces of the samples in Set 1 were observed at the region adjacent to the top coat/bond coat interface; the failure mode was adhesive. Although an equal number of three samples was used for each set for thermal cycling and tensile adhesion tests, statistical analysis (two tailed t-test with a 95% confidence interval) indicates that the mean ultimate tensile stress of the samples in Set 1 is significantly lower than that of the samples in Set 3, and there is no difference in the mean ultimate tensile stress between the samples in Sets 2 and 3.[4]

The fracture surfaces at the substrate side after the tensile adhesion tests are shown in Fig. 2(a), (b), and (c) for samples from Sets 1, 2, and 3, respectively. Because the fracture surface of the samples in Set 1 was close to the top coat/bond coat interface, its fracture course followed a relatively flat contour of the bond coat/substrate. Consequently, the fracture surface of the sample in Set 1 is smoother than those of the samples in Sets 2 and 3. The surface roughness (R_a) was found to be 14.5 ± 0.5 μm for the samples from Set 1, which is lower than those of the samples from Set 2 (16.7 ± 0.3 μm) and the samples from Set 3 (15.7 ± 0.4 μm). Furthermore, the bond coat elements of nickel, chromium, and aluminum were detected by EDAX in the sample from Set 1 (the region is indicated by the arrows).

Topographic features of the fracture surfaces of the samples in Sets 1 and 2 are different from those of the samples in Set 3. More localized tearing is present in the samples of Sets 1 and 2. This may indicate that a microcrack network was formed during initial thermal cycling. This type of microcracking had no detrimental effect on the thermal cycling lifetime of thermal barrier coatings.[5] Although the topographic features of the fracture surfaces of the samples in Sets 2 and 3 were not identical, and the thermal history was not the same, the ultimate tensile stress, in fact, was comparable.

In another study,[6] the adhesion strength of the plasma-sprayed coatings (yttria-stabilized zirconia top coat on a steel substrate without bond coat) was reduced by 25% after heat treatment at 1150 °C for 10 h was carried out. When a NiCrAlY bond coat was applied between the top coat and the substrate, the fracture locus was shifted to the top coat away from the interface, and the strength was significantly increased. These experimental results are consistent with the current findings that thermal processes (either by thermal cycling or heat treatment) degrade coating adhesion strength when a suitable bond coat is not applied.

The difference in average ultimate tensile stress of the samples in Sets 1 and 2 is most likely due to thermal mismatch stress

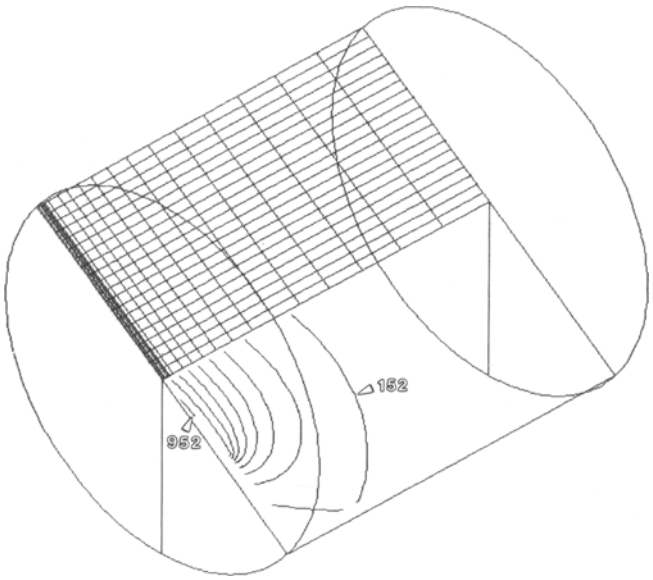

Fig. 3 Finite-element representation of the mesh and temperature distribution within a tensile adhesion test specimen. Only the coating system and the substrate plug are shown. The upper part of the diagram indicates the mesh that was used; the closer spacing of lines represents the bond coat and top coat. The lower half of the figure indicates the temperature contours along the mid-plane (length orientation) of Set 1 specimens at the thermal equilibrium condition during heating. The isothermal lines are in increments of 100 °C.

at the top coat/bond coat interface region. The bond coat of the samples in Set 2 contains 40% (by volume) silicates, which lead to a lower thermal mismatch stress during thermal cycling and less microcracking at the interface, resulting in a higher ultimate tensile stress and a fracture plane within the top ceramic coat. In the case of Set 1, a high thermal mismatch stress contributes to microcrack formation along the top ceramic coat in the vicinity of the top coat/bond coat interface, resulting in a lower ultimate tensile stress and a fracture plane along the interface. The thermal mismatch stress at the interface is due to differences in coefficients of thermal expansion of the coatings and the temperature nonuniformity during thermal cycling. This stress was acting parallel to the coating surface and would open cracks by a shearing mechanism.[7] During thermal cycling, when the shear stress exceeded the fracture stress of the top coat, microcracks may have initiated and propagated along the interface. This in turn degraded the fracture strength of the top coat and, consequently, resulted in decreased ultimate tensile stress in the subsequent tensile adhesion tests.

The thermal mismatch stress at the top coat/bond coat interface is estimated using a calculated temperature field and coefficient of thermal expansion. The coefficient of thermal expansion of bulk zirconia range from 9 to 11×10^{-6}/K.[8] The coefficient of thermal expansion of plasma-sprayed yttria partially stabilized zirconia is 10×10^{-6}/K,[9] which was used in the calculation for the top coat in this study. The measured average coefficients of thermal expansion (25 to 1030 °C) of the NiCrAl and NiCrAl/bentonite sintered compacts were found to be 19.8 and 13.6×10^{-6}/K, respectively. A thermal coefficient of expansion of 17.1×10^{-6}/K was used for the HX substrate.[10]

The temperature field was calculated by solving the energy equation for heat conduction in the samples using the Phoenis code.[11] Because the temperature gradient was more significant in the front where heating was applied, finer grids were used. The grids are shown in the top half of the cross section along the cylinder axis in Fig. 3. The other half of the figure shows the temperature field in a sample of Set 1 at a thermal equilibrium condition during heating. The calculated thermal mismatch stresses indicate that the stress is 40% lower for the samples in Set 2 compared to those in Set 1.

In Ref 12, a metallic bond coat (identical to that used in Set 1) was recommended for high-temperature practical applications at 980 °C, presumably without significant oxidation. In the present study, thermal cycling lasted only 7 h at 960 °C, and hence, oxidation of the metallic components in the bond coat and the substrate could not contribute to the degradation of bond strength. It would be interesting to investigate the bond strength obtained by the tensile adhesion tests as a function of the number of thermal cycles. In this way, the thermal barrier coating failure process due to thermal mismatch of the system, and due to oxidation of bond coat and/or substrate, could be distinguished and monitored.

4. Conclusions

Thermal cycling combined with tensile adhesion tests were applied to two types of thermal barrier coatings. It was found that degradation in bond strength and failure mode can be related to the composition of the bond coat. The different coefficients of thermal expansion of the bond coats resulted in different thermal mismatch stress levels at the top ceramic coat/bond coat interface.

Acknowledgment

The authors gratefully acknowledge helpful discussions with Ken Reid, experimental assistance from David Allan, and the management of Sherritt Gordon Ltd. for permission to publish this work.

References

1. ASTM Designation C633, Standard Test Method for Adhesion or Cohesive Strength of Flame-Sprayed Coatings, *Annual Book of ASTM Standards*, Vol 02.05, American Society for Testing and Materials, 1989, p 663-667
2. S. Stecura, "Effects of Compositional Changes on the Performance of Thermal Barrier Coating System," NASA TM-78976, Aug 1978
3. H. Wang, H. Herman, G.A. Bancke, and M. Wood, Flame Rig Testing of Thick Thermal Barrier Coatings, *Protective Coatings: Processing and Characterization*, R.M. Yazici, Ed., TMS, 1990, p 155-163
4. R.E. Walpole and R.H. Myers, *Probability and Statistics for Engineers and Scientists*, 2nd ed., Macmillan Publishing, 1978, p 202-205
5. N.R. Shankar, C.C. Berndt, H. Herman, and S. Rangaswamy, Acoustic Emission from Thermally Cycled Plasma-Sprayed Oxides, *Am. Ceram. Bull.*, Vol 62, 1983, p 614-619
6. N.R. Shankar, C.C. Berndt, and H. Herman, Characterization of the Mechanical Properties of Plasma-Sprayed Coatings, *Advances in Materials Characterization*, D.R. Rossington, R.A. Condrate, and R.L.Snyder, Ed., Plenum, 1983, p 473-489
7. C.C. Berndt and H. Herman, Anisotropic Thermal Expansion Effects in Plasma-Sprayed ZrO_2-8%-Y_2O_3 Coatings, *Ceram. Eng. Sci. Proc.*, Vol 4 (No. 9/10), 1983, p 792-801
8. V.J. Tennery, *Ceramic and Components for Engines*, American Ceramic Society, 1989, p 148-194
9. S. Rangaswamy, H. Herman, and S. Safai, Thermal Expansion Study of Plasma-Sprayed Oxide Coatings, *Thin Solid Films*, Vol 73, 1980, p 42-52
10. *Metals Handbook*, Properties and Selection: Stainless Steels, Tool Materials and Special-Purpose Metals, Vol 3, 9th ed., American Society for Metals, 1979, p 312
11. J.C. Ludwig and D.B. Spalding, "The Phoenis Reference Manual," CHAM TR/200, CHAM Ltd., London, England, 1990
12. "Metco 443 and Metco 443NS Nickel Chromium/Aluminum Composite Powders," Technical Bulletin, Apr 1986, Metco Inc., Westbury, NY, p 10-130